

# Four-Channel 784 Gbit/s Transmitter Module Enabled by Photonic Wire Bonding and Silicon-Organic Hybrid Modulators

M. R. Billah<sup>(1,2)</sup>, J. N. Kemal<sup>(1)</sup>, P. Marin-Palomo<sup>(1)</sup>, M. Blaicher<sup>(1,2)</sup>, Y. Kutuvantavida<sup>(1)</sup>, C. Kieninger<sup>(1)</sup>, H. Zwickel<sup>(1)</sup>, P.-I. Dietrich<sup>(1,2,4)</sup>, S. Wolf<sup>(1)</sup>, T. Hoose<sup>(1,2)</sup>, Y. Xu<sup>(1)</sup>, U. Troppenz<sup>(3)</sup>, M. Moehrle<sup>(3)</sup>, S. Randel<sup>(1)</sup>, W. Freude<sup>(1)</sup>, C. Koos<sup>(1,2,4)</sup>

<sup>(1)</sup> Institute of Photonics and Quantum Electronics (IPQ), Karlsruhe Institute of Technology (KIT), Engesserstrasse 5, 76131 Germany, [muhammad.billah@kit.edu](mailto:muhammad.billah@kit.edu), [christian.koos@kit.edu](mailto:christian.koos@kit.edu)

<sup>(2)</sup> Institute of Microstructure Technology (IMT), KIT, Hermann-von-Helmholtz-Platz 1, 76344 Germany

<sup>(3)</sup> Fraunhofer Institut for Telecommunications, Heinrich Hertz Institute (HHI), Einsteinufer 37, 10587 Germany

<sup>(4)</sup> Vanguard Photonics GmbH, Karlsruhe, Germany

**Abstract** We demonstrate a four-channel hybrid multi-chip module comprising InP lasers, silicon-organic hybrid (SOH) modulators, and single-mode fibers, all connected via photonic wire bonds. We transmit 56 GBd QPSK and 16QAM signals at a total data rate of 784 Gbit/s over 75 km.

## Introduction

High-speed coherent transmission is key to overcome transmission bottlenecks in metro networks and data-center interconnects. For cost-efficient and compact implementation of coherent transceivers, the silicon photonic (SiP) integration platform is particularly attractive, exploiting the vast advantages of CMOS-based fabrication<sup>1</sup> and photonic-electronic co-integration<sup>2</sup>. However, technical implementation of SiP transceivers still suffers from fundamental restrictions such as the lack of efficient on-chip light sources and the rather low efficiency of SiP in-phase/quadrature (IQ) modulators. Regarding light sources, despite tremendous progress in heterogeneous integration of III-V dies on SiP substrates<sup>3</sup>, commercial products still use external lasers that are coupled to the SiP chip<sup>4,5</sup>. These concepts rely on expensive active alignment, thereby spoiling most of the scalability advantages of the SiP platform. With respect to IQ modulators, the main problem is the low efficiency of *pn*-depletion-type phase shifters<sup>6</sup>, leading to rather large  $U_{\pi}L$  products of typically more than 10 Vmm. The highest single-polarization line rate (net data rate) of a SiP IQ modulator amounts to 227 Gbit/s (154.1 Gbit/s), generated by a standalone device that was fed by a benchtop-type laser<sup>7</sup>. For coherent transmitter modules with co-integrated light source, the highest line rate (net data rate) amounts to<sup>8</sup> 40 Gbit/s (33.3 Gbit/s).

In this paper we demonstrate that the restrictions of the SiP platform can be overcome by merging two hybrid integration approaches: We exploit the technique of silicon-organic hybrid (SOH) integration<sup>9</sup>, which is particularly well suited for high-speed IQ modulators<sup>10,11,20</sup>, and combine it with the concept of hybrid multi-chip integration, which is enabled by photonic wire bonding<sup>12,15</sup>, to simultaneously overcome the light-source and the modulation-efficiency challenge in silicon photonics. We demonstrate a four-channel transmitter enabling 56 GBd 16-state quadrature amplitude modulation (16QAM) transmission on three channels and quadrature phase-shift keying (QPSK) on the fourth channel. To the best of our knowledge, this is the first demonstration of multi-channel coherent transmission from a SiP module with hybrid integrated light source. The total data rate (line rate) amounts to 784 Gbit/s (732.7 Gbit/s), transmitted over 75 km. This is the

highest data rate demonstrated by a SiP transmitter module with co-integrated lasers to date, exceeding our own previous record<sup>16</sup>. We believe that our experiments mark an important step towards hybrid integration of powerful chip-scale wavelength-division multiplexing (WDM) transceivers that overcome the deficiencies of the SiP platform and that can handle multi-terabit/s data rates.

## Hybrid integration approaches

Our hybrid multi-chip module (MCM) is illustrated in Fig. 1(a). For chip-chip and fiber-chip coupling, we exploit the technique of photonic wire bonding<sup>12-15</sup>, which relies on advanced three-dimensional (3D) nano-printing of single-mode connections between coarsely positioned chips in a fully automated process. Photonic wire bonding is particularly well suited for connecting SiP circuits to highly efficient InP light sources<sup>14,15</sup>. This approach is complemented by SOH integration, which combines the unique processing advantages of silicon photonics with the wealth of optical properties obtained by theory-guided molecular design of organic materials<sup>8-11,17-20</sup>. The SOH concept enables highly efficient modulators with  $U_{\pi}L$  products down to<sup>17</sup> 0.5 Vmm. The devices offer ultra-low energy consumption<sup>17</sup> and enable high-speed coherent<sup>10,11</sup> and non-coherent<sup>18,19</sup> transmission with single-polarization line rates of up to<sup>20</sup> 400 Gbit/s (100 GBd 16QAM). The high modulation efficiency allows to drive SOH devices directly from binary CMOS outputs of field-programmable gate arrays (FPGA) without digital-to-analogue converters (DAC) or drive amplifiers<sup>21</sup>. The MCM used for our experiment consists of a SiP die comprising an array of four IQ modulators, each built from two nested SOH Mach-Zehnder modulators (MZM), Fig. 1(a). The devices are fed by an array of horizontal-cavity surface-emitting lasers (HCSEL) containing InGaAsP distributed-feedback structures with etched 45° mirrors to deflect the light to a surface-normal direction<sup>22</sup>. The HCSEL emit at wavelengths near 1550 nm and are placed side by side with the SiP die on a common submount. In contrast to lasers mounted to the top surface of the SiP chip, this configuration allows for thermal decoupling and efficient cooling of the laser. The basic structure of an SOH MZM is illustrated in Fig. 1(b). Each MZM comprises two SOH phase modulators (PM) that are driven by a single coplanar

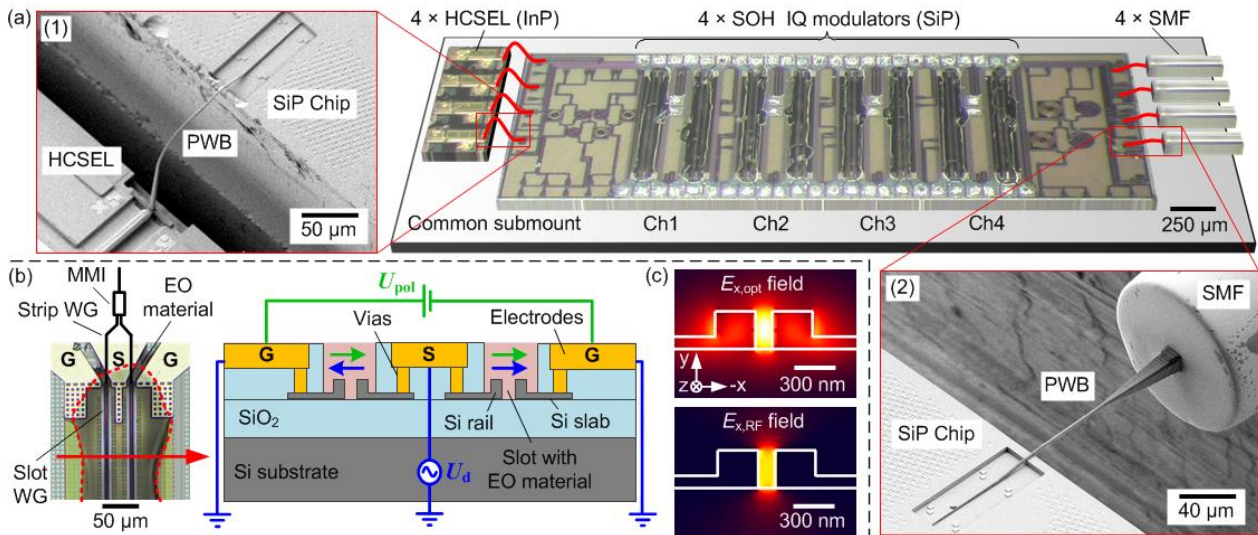


**Fig. 1:** Concept of hybrid integration on chip and package level. **(a)** Four-channel multi-chip-module (MCM) comprising InP horizontal-cavity surface emitting lasers (HCSEL), silicon-organic hybrid (SOH) modulators, and single mode fibers (SMF), all connected with photonic wire bonds (PWB). Inset (1) shows a PWB connecting a HCSEL to the SiP chip<sup>13</sup>, Inset (2) refers to a PWB between the SiP chip and an SMF. **(b)** Top view of an SOH MZM after local deposition of the organic EO material (red contour) with a schematic of the device cross section. The MZM consists of two slot-waveguide (WG) phase modulators, driven in push-pull operation by a single coplanar GSG transmission line. Before and after the modulator sections, the light is split and combined by multimode interference couplers (MMI). **(c)** Cross-sectional view and simulated distribution of the dominant electrical component  $E_x$  of the optical quasi-TE mode field and the RF mode field for a single phase modulator. Both fields show good overlap, resulting in highly efficient modulation.

ground-signal-ground (GSG) transmission line. Each PM consists of a slot waveguide, covered by an organic EO material. The slot waveguide leads to a strong overlap of the optical mode with the modulating RF field<sup>9</sup>, Fig. 1(c), and hence high modulation efficiency. The basic SiP waveguide structures are fabricated by widely available CMOS processes, and the organic EO material is deposited in a post-processing step. In our experiments, the data signals are coupled to four single-mode fibers, which can be replaced by a WDM multiplexer in the future. The photonic MCM is assembled in several steps: First, chips and fibers are mounted on a common carrier with low precision. Negative-tone resist (IP-Dip<sup>TM</sup>, Nanoscribe GmbH) is then drop-cast onto the assembly. Machine-readable alignment features on the optical chips define the photonic wire bond (PWB) start and end point. PWB are fabricated through two-photon polymerization (TPP)<sup>11</sup>. The structures are developed in propylene-glycol-methyl-ether-acetate (PGMEA). Insets (1) and (2) of Fig. 1(a) show fabricated PWB, both for the laser and the fiber interface. Exploiting the freedom of TPP-written 3D structures, PWB can be tapered to exactly match the mode fields of the connecting waveguides.

After PWB fabrication, the organic EO material is locally deposited on the slot waveguides, Fig. 1(b). To avoid contact of the organic EO cladding with the PWB, we developed a high-precision dispensing technique enabling trace widths of less than  $20\ \mu\text{m}$  – a key step to combine SOH integration with photonic wire bonding. To induce macroscopic EO activity, the material is poled by heating it to the glass-transition temperature while applying a DC voltage  $U_{\text{pol}}$  between the floating ground electrodes of the MZM. The resulting poling fields in the slots align<sup>17</sup> the dipolar chromophores as indicated by the green arrows in Fig. 1(b). While keeping the poling voltage, the chip is cooled back to room temperature such

that the acentric order of the chromophores is conserved. The orientation of the RF modulation field (blue arrows in Fig. 1(b)) results in efficient push-pull operation<sup>9</sup>. The  $U_{\pi}L$  product measured in this module is  $1.3\ \text{Vmm}$ . This is bigger than the values published earlier<sup>17</sup> since the EO material (SEO100) was chosen for good thermal stability enabling, e.g., operation<sup>22</sup> at  $80\ ^\circ\text{C}$ , rather than for highest EO coefficient<sup>23</sup>. After poling, we estimate the losses of the PWB interfaces by measuring the power levels  $P_{\text{launch}}$  at the output SMF and comparing it to the emission power  $P_{\text{out}}$  of the HCSEL prior to photonic wire bonding. Using the measured SOH MZM device loss of 8 dB, we find the lowest insertion loss of 3.9 dB for a PWB connecting the HCSEL to SiP chip and of 5.4 dB for the PWB connecting the SiP to the SMF. These values leave vast room for further improvement – PWB between a SiP chip and a multi-core fiber<sup>13</sup> have been demonstrated with insertion losses down to 1.7 dB. The increased losses in this experiment are due to a slight over-etch of the inversely tapered SiP waveguides and due to the fact that the PWB were not yet overlaid, as assumed in their design. To estimate the uniformity of the PWB, we measure the launch power  $P_{\text{launch}}$  in the SMF for maximum transmission of the modulators. The highest  $P_{\text{launch}} = -11.6\ \text{dBm}$  is found in channel 4 (Ch4) and the lowest is Ch1 with  $-19.9\ \text{dBm}$ . The deviation is caused by a dirt particle sticking on the PWB on the HCSEL side, leading to reduced performance of this channel.

### Data transmission experiments

For the transmission experiments, we use the setup shown in Fig. 2(a). An arbitrary-waveform generator (AWG) provides the RF signals to the IQ modulators through GSG probes. Both transmission lines are terminated with  $50\ \Omega$ . We transmit random IQ signals with a pre-equalization obtained through the measured frequency response of each modulator.



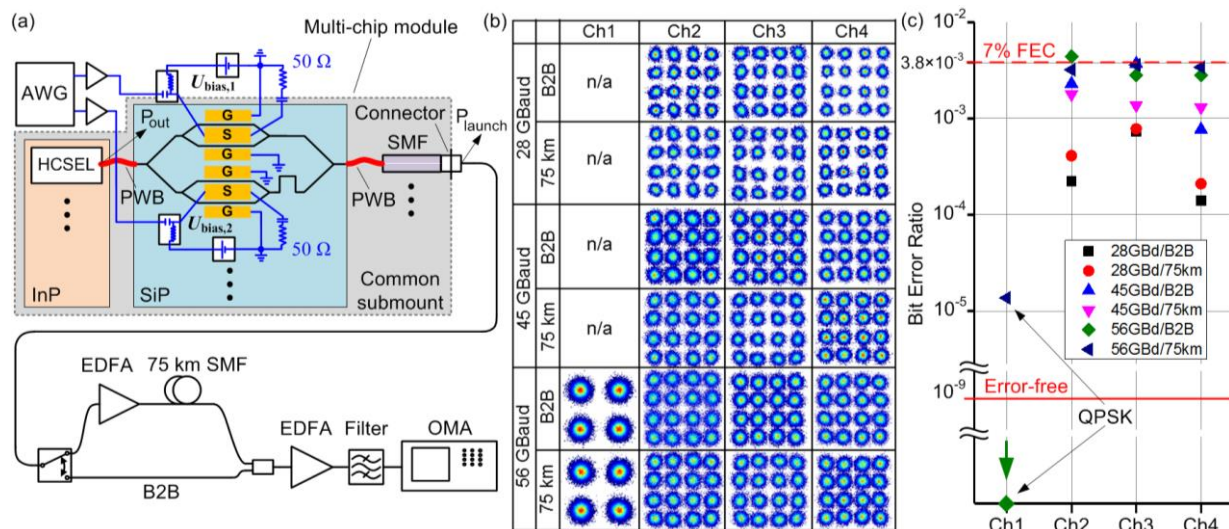


**Fig. 2:** Coherent transmission experiments. **(a)** Transmission setup for measuring one channel at a time. **(b)** Constellation diagrams for transmission of all channels at 28 GBd, 45 GBd, and 56 GBd. The performance of Ch1 was impeded by a dirt particle on one of the PWB, leading to a lower launch power, such that only QPSK transmission was successful. **(c)** Measured bit error ratio (BER) for all channels. All BER values stay below the threshold for 7% FEC except for the 56 GBd back-to-back operation (B2B) of Ch2. Since the 75 km result is below the FEC limit, we attribute this result to a non-optimum adjustment of the modulator bias. The aggregate module line rate amounts to 784 Gbit/s.

The length of the pseudo-random bit sequence (PRBS) amounts to  $2^{11}-1$ . The optical signal is sent either back-to-back (B2B) or through a 75 km long SMF. The signals are coherently received using an optical modulation analyzer (Keysight N4391) along with pre-amplifier. The summary of recorded constellation diagrams is shown in Fig. 2(b). As expected, Ch4 shows the cleanest constellation diagrams, whereas Ch1 is able to transmit QPSK only. We calculate the bit error ratio (BER) for each constellation diagram, Fig. 2(c). Note that for Ch2, the B2B BER is worse than the one for the 75 km transmission – we attribute this to non-optimum adjustment of the bias point in the B2B experiment. All other BER are below the limit for second-generation hard-decision forward-error correction (FEC) with 7% overhead. This leads to an aggregate line rate (net data rate) of 784 Gbit/s (732.7 Gbit/s) – the highest values so far demonstrated by a SiP transmitter module with hybrid integrated lasers. The per-channel line rates (net data rates) amount to 224 Gbit/s (209 Gbit/s) per polarization – on par with (exceeding) the highest line rates (net data rates) demonstrated with unpackaged standalone SiP depletion-type modulators<sup>7</sup>.

### Summary

We demonstrate a four-channel coherent transmitter module that combines hybrid multi-chip integration of SiP circuits and InP lasers with hybrid on-chip integration of organic EO materials to overcome the two dominant performance restrictions of the SiP platform. We demonstrate aggregate line rates of up to 784 Gbit/s over 75 km. To the best of our knowledge, this is the highest line rate demonstrated with a SiP transmitter module with hybrid lasers.

This work was supported by the EU-FP7 project BigPIPES, the European Research Council (ERC Starting Grant ‘EnTeraPIC’, # 280145), the BMBF joint project PHOIBOS, the Alfred Krupp von Bohlen und Halbach Foundation, the Helmholtz International Research School for Teratronics (HIRST), Karlsruhe School of Optics & Photonics (KSOP), and the Karlsruhe Nano-Micro Facility (KNMF).

### References

- [1] Pavesi, D. Lockwood, *Silicon Photonics III: Systems and Applications*. Vol. 122. Springer Sci. & Business Media, 2016.
- [2] Sun *et al.* “Single-chip microprocessor that communicates directly using light”, *Nature* **528**, 534-538 (2015).
- [3] Z. Wang *et al.* “A III-V-on-Si ultra-dense comb laser,” *Light: Science & Applications* **6**, e16260 (2017)
- [4] N. Hatori *et al.* “A Hybrid Integrated Light Source on a Silicon Platform Using a Trident Spot-Size Converter,” *J. Lightwave Technol.*, **32**, 1329-1336 (2014).
- [5] Snyder *et al.* “Hybrid integration of wavelength-tunable laser with a silicon photonic integrated circuit” *J. Lightw. Tech.* **31**, 3934-42 (2013).
- [6] J. Fujikata *et al.* “Record-high Modulation-efficiency Depletion-type Si-based Optical Modulator with In-situ B Doped Strained SiGe Layer on Si Waveguide for 1.3  $\mu\text{m}$ ,” *ECON 2016*, paper Tu.3.A.4.
- [7] Fang *et al.* “Silicon IQ Modulator Based 480km 80x453.2GB/s PDM-eOFDM Transmission on 50GHz Grid with SSMF and EDFA-only Link,” *OFC 2015*, paper M3G.5 (2015).
- [8] de Valicourt *et al.* “80Gb/s PDM-QPSK PIC-to-PIC Transmission based on Integrated Hybrid Silicon/III-V Wavelength-tunable Transmitter and Monolithic Silicon Coherent Receiver”, *OFC 2017*, Tu2L.2.
- [9] Koos *et al.* “Silicon-Organic Hybrid (SOH) and Plasmonic-Organic Hybrid (POH) Integration,” *J. Lightwave Technol.* **34**, 256-268 (2016).
- [10] Lauerermann *et al.* “Low-power silicon-organic hybrid (SOH) modulators for advanced modulation formats,” *Opt. Express* **22**, 29927-36 (2014).
- [11] Lauerermann *et al.* “40 GBd 16QAM Signaling at 160 Gb/s in a Silicon-Organic Hybrid Modulator,” *J. Lightw. Technol.* **33**, 1210-1216 (2015).
- [12] Lindenmann *et al.* “Photonic wire bonding: a novel concept for chip-scale interconnects,” *Opt. Express* **20**, 17667-17677 (2012).
- [13] Lindenmann *et al.* “Connecting silicon photonic circuits to multi-core fibers by photonic wire bonding. *J. Lightw. Technol.* **33**, 755-765 (2015).
- [14] Billah *et al.* “Multi-chip integration of lasers and silicon photonics by photonic wire bonding”. *CLEO, Stu2F.2* (2015).
- [15] Hoose *et al.* “Multi-Chip Integration by Photonic Wire Bonding: Connecting Surface and Edge Emitting Lasers to Silicon Chips,” *OFC 2016*, paper M2L.7 (2016).
- [16] Billah *et al.* “8-channel 448 Gbit/s silicon photonic transmitter enabled by photonic wire bonding”, *OFC2017*, paper Th5D.6 (2017).
- [17] Koeber *et al.* “Femtojoule electrooptic modulation using a silicon-organic hybrid device,” *Light: Sci. & Appl.*, **4**, e255, 2015.
- [18] Zwickel *et al.* “Silicon.organic hybrid (SOH) modulators for intensity-modulation/direct-detection links with line rates of up to 120 Gbit/s,” *Opt. Express*, accepted (2017).
- [19] Wolf *et al.* “Silicon-Organic Hybrid (SOH) IQ Modulator for 100 GBit/s On-Off Keying,” submitted to ArXiv (2017).
- [20] Wolf *et al.* “Silicon-Organic Hybrid (SOH) IQ Modulator for 100 GBd 16QAM Operation,” *OFC, Paper Th5C.1* (2017).
- [21] Wolf *et al.* “DAC-less amplifier-less generation and transmission of QAM signals using sub-volt silicon-organic hybrid modulators,” *J. Lightwave Technol.* **33**, 1425-1432, (2015).
- [22] Moehrl *et al.* “Ultra-low threshold 1490 nm surface-emitting BH-DFB laser diode with integrated monitor photodiode”, *ICIPRM 1-4* (2010)
- [23] Lauerermann *et al.* “Generation of 64 Gbd 4ASK signals using a silicon-organic hybrid modulator at 80°C,” *Opt. Expr.* **24**, 9389-9396 (2016).